

Photogrammetric 3D modelling and experimental archaeology reveals new technological insights into engraved soapstone sinker production in Western Norway (6400-3300 cal. BC)

Simon Radchenko^{a,*}, Mette Adegeest^b, Aimée Little^c, Anja Mansrud^b, Morten Kutschera^d

^a Museum of Archaeology, University of Stavanger, Erik Aanestads vei, 12, Randaberg, 4070, Norway

^b Museum of Archaeology, University of Stavanger, Norway

^c Centre for Artefacts and Materials Analysis, Department of Archaeology, University of York, England

^d Agder Fylkeskommune, Norway

ARTICLE INFO

Keywords:

Photogrammetry
Actualistic experiment
Soapstone
Sinker
Late mesolithic
Early neolithic

ABSTRACT

This pilot research presents the first study integrating digital submillimetre image-based 3D modelling with experimental archaeology to examine how soapstone sinker stones, dated to the late Mesolithic and early Neolithic periods in Western Norway (6400-3300 cal. BC), were manufactured and engraved. Photogrammetry was used as a bridging method to compare archaeological artefacts and experimental data. Applying the same high-accuracy digital solutions to five archaeological and 26 experimentally commissioned replica sinkers, permitted linking characteristic features of engraved surfaces with specific tools and techniques. This enabled identifying and distinguishing flint-made surface modifications from quartz, bone and sandstone, and revealed novel information on key aspects of the sinker's biographies and *chaîne opératoire*, including the initial shaping of the blank by means of grinding stones, the relative chronology of the engraving process, and damage to the artefact surface caused during use-life and via post-deposition processes. This study suggests that the central furrow on the soapstone sinkers, assumed to function for fastening a line, was produced in a consistent way, likely with quartz tools, while other incisions showed more variation. Aesthetic concerns are one possible reason for these differences, though others should be considered; future studies may help provide greater insight into the reasons driving this preference.

1. Introduction

This paper reports on the first study integrating digital submillimetre image-based 3D modelling with experimental archaeology to examine how soapstone sinker stones, dated to the late Mesolithic and early Neolithic periods in Western Norway (6400-3300 cal. BC), were manufactured and engraved. Small soapstone implements, sometimes referred to as “coffee-bean sinkers” due to their characteristic oval shape and central lengthwise furrow, are a distinctive artefact type uniquely distributed along the Atlantic coast of Western and Southwestern Norway between c. 6400-3300 cal. BC (Figs. 1 and 2). The central furrow is assumed to allow attachment to a line, hence why these items are commonly interpreted as sinker stones used for fishing. Sinker stones, also known as fishing weights, are usually attached to the fishing line

above the hook. The weight helps to lower and secure a baited hook down to the desired depth, which can be crucial for targeting specific species of fish that feed at particular levels in the water. It is presumed that Mesolithic and Neolithic sinkers were used in combination with small bone fishhooks for line-fishing in shallow water (Åstveit, 2008, 573; Bergsvik, 2017: 81–84; Skjelstad, 2003). When retrieved from verifiably dated archaeological contexts, soapstone coffee-bean sinkers (hereafter referred to as bean sinkers) most often occur at Late Mesolithic sites, or from mixed Late Mesolithic and Early Neolithic occupation layers (Bjørge, 1981: 107–108, 113; Bergsvik, 2017: 81). They also appear as undated stray finds (Bergsvik, 2017: 75, 86). In total, more than 500 artefacts have been classified as bean sinkers in the Norwegian national database of university museum collections. Most have an oval shape, are less than 2 cm in length and weigh less than 10 g, but larger

* Corresponding author.

E-mail address: Simon.radchenko@gmail.com (S. Radchenko).

<https://doi.org/10.1016/j.daach.2025.e00427>

Received 25 June 2024; Received in revised form 20 February 2025; Accepted 26 April 2025

Available online 30 April 2025

2212-0548/© 2025 The Authors. Published by Elsevier Ltd. This is an open access article under the CC BY license (<http://creativecommons.org/licenses/by/4.0/>).

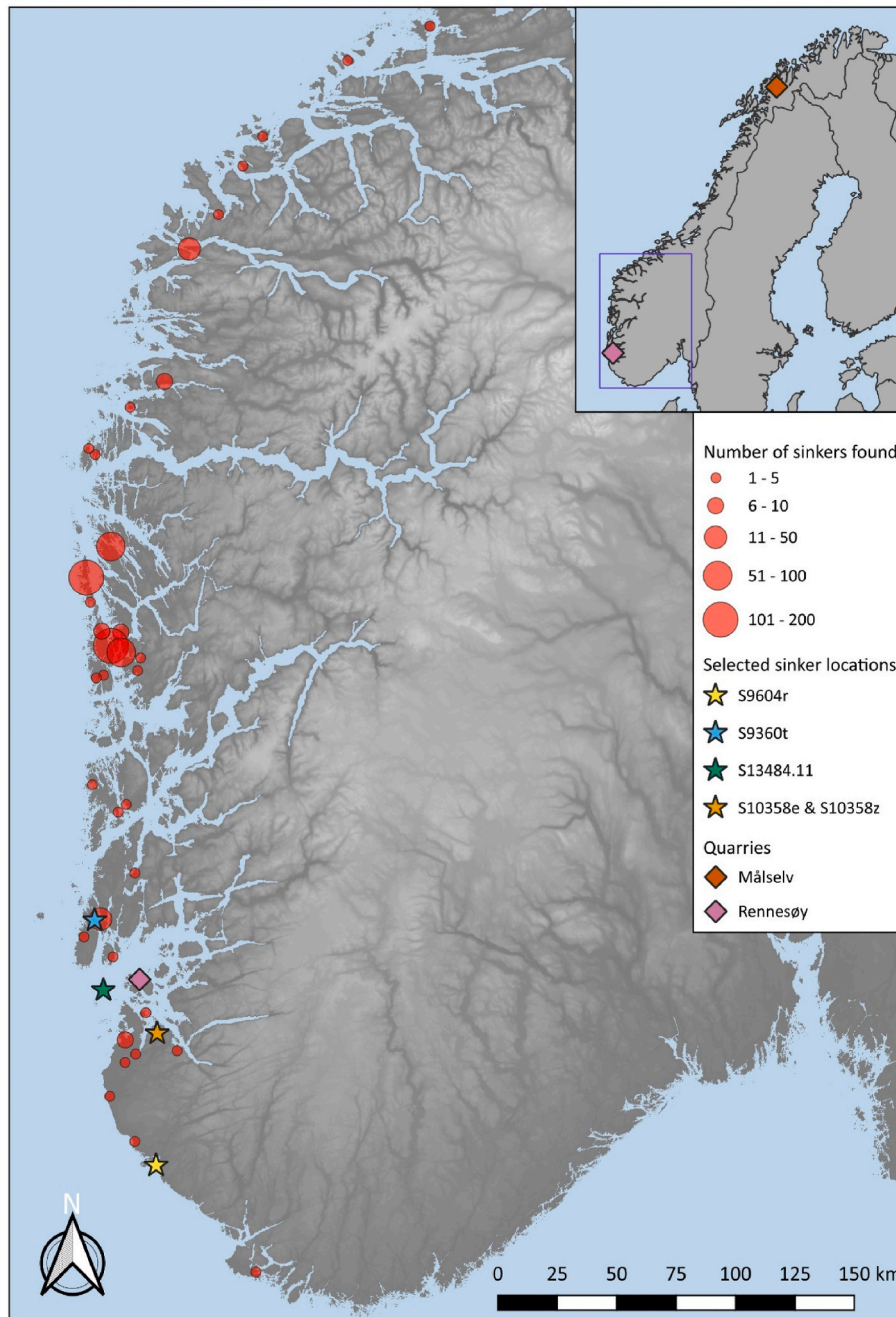


Fig. 1. Map with geographical distribution and frequency of all soapstone bean sinkers attributed to the Late Mesolithic and/or Early Neolithic. Find locations of the specific sinkers discussed in the text (see Fig. 2) and quarry locations of the soapstone used in the experiments are highlighted (map: Mette Adegeest).



Fig. 2. Five engraved “coffee-bean sinkers” from Rogaland were examined in this study (photo: Annette Græsli Øvrelid, AM-UIS).

Table 1

Basic data for the five selected archaeological sinkers.

Artefact ID.	Municipality	Find year	Find method	Attributed to	Dating method
S9360t	Karmøy	1968	Surface collection	Late Mesolithic - Neolithic	Assemblage typology
S9604r	Eigersund	1971	Excavation	Neolithic	Assemblage typology
s10358e	Sandnes	1988	Excavation	Late Mesolithic	C14
s10358z	Sandnes	1988	Excavation	Late Mesolithic	C14
S13484.11	Kvitsoy	2015	Excavation	Late Mesolithic - Late Neolithic	C14

and more irregular examples have also been registered (Bergsvik, 2017). This paper focuses on the small sinkers (>10g), a dataset of 387 artefacts.

The bean sinkers are occasionally more elaborately engraved with criss-cross-patterns and other geometric designs, multiple crosswise furrows, and/or side notches (Fig. 1). This concerns 14 % of the small sinkers. Most researchers assume these surface modifications are purely ornamental (summarised in Bergsvik, 2017: 86–89), whilst some have suggested possible technological functions (Bjørge, 1981: 111). Early archaeological debate has further questioned whether these objects are too small and lightweight to have functioned as sinkers for line fishing and proposed an alternative interpretation as amulets or pendants (Bøe, 1925, 1934; Bakkevig, 2021). Soapstone is soft and easy to carve, which may be why various other types of engraved soapstone artefacts such as hatchets and mace heads occur across Southern Norway during the Mesolithic period (Glørstad, 2002).

So far, basic information about how soapstone artefacts and associated engravings were made, and what tools were used to produce them, is lacking. It has been suggested that lithic blades or flakes and/or grinding stones may have been employed to make the engravings, and at some excavated sites, pieces of soapstone, possibly representing crafting debris, have been noted (Bergsvik, 2017: 79, 86). Until now, no experimental research has tested this theory or produced empirical datasets vital for cross-referencing and interpreting archaeological specimens.

The primary objective of this study was to obtain novel information on how the sinkers and the furrows/grooves were manufactured. By integrating experimental archaeology and image-based 3D modelling, we aim to: 1. advance current understandings of production techniques; 2. identify the tools employed in making the furrows and grooves; 3. distinguish intentional engravings from surface modifications caused by erosion or use; and by extension, 4. make advancements in the field of digital imaging techniques by applying these methods to engraved soapstone artefacts for the first time.

We provide here a digital study of engraved soapstone surfaces, employing technological solutions grounded in image-based 3D modelling, and the post-processing of high-polygonal surfaces, undertaken on archaeological finds and experimentally commissioned sinkers. By studying the submillimetre variations in experimentally produced objects and archaeological artefacts in tandem, we aim to establish a link between the morphology of engraved surfaces and the engraving technology, opening the possibilities for applying these methods and knowledge to a wider dataset. By doing so, we aim to deepen our understanding of this understudied category of engraved Mesolithic objects and push the current trends in 3D-modelling of stone artefacts forward.

3D modelling of archaeological artefacts offers a useful method for capturing information on different aspects of production techniques, sometimes even use and post-depositional damage. Rarely, however, is this information alone sufficient to make detailed interpretations regarding specific modes of manufacture, use etc. Like use-wear analysis (see Bamforth, 2010; Van Gijn, 2010), 3D modelling of artefact surfaces, we argue, requires cross-checking with 3D models of experimentally replicated artefacts.

In this paper we show how 3D studies of experimental datasets provide valuable comparative reference data for interpreting soapstone technology. We present results of a digital study combined with

actualistic experiments – an approach which recreates past practices by employing methods and materials known to have been available to the people/time period studied (Outram, 2008; Nami, 2010; Lin et al., 2018). To this end, replicas of Mesolithic tools (discussed in more detail below) commonly found on Norwegian Mesolithic and Early Neolithic sites from Western Norway (Bjerck, 2010; Damlien et al., 2024; Nyland, 2016; Skjelstad, 2003) were used to manufacture the sinkers and the engravings. Our hypothesis asserted that by integrating 3D and (actualistic) experimental methods of sinker production it is possible to identify different (broad) categories of soapstone sinker-making tools. Experiments were executed to assess whether the shape and depth of the engravings produced on replica soapstone sinkers could demonstrably be shown to correspond with those visible on the artefacts. Drawing on earlier suggestions (Bergsvik, 2017: 79, 86) that grinding stones were possibly used in the production process, we further aimed to investigate whether surface traces of grinding and polishing from manufacture could be visualised and documented on the experimentally produced replicas. Essentially, by comparing high-resolution digital images of surface information on archaeological and experimentally produced sinkers, we aimed to establish the manufacture- and engraving stages of the bean sinker *chaîne opératoire*. Finally, we wanted to see whether it was possible to identify soapstone debris resulting from the manufacturing process as a means of potentially identifying not only the toolkits but also *in situ* production spaces in the future, as achieved for other Northwestern European Mesolithic artefacts, such as axes (e.g., Carlsson, 2007; Eymundsson et al., 2018; Conneller et al., 2018) and bone tools (Molin and Gummeson, 2021).

2. Material and methods

2.1. Archaeological and experimental materials

Five archaeological sinkers from Rogaland were digitized and analysed (Fig. 2; Table 1). These were selected as being representative of the overall type (bean-shaped with a central furrow) and for displaying a variety of surface modifications, including perpendicular grooves, criss-cross patterns and side-notches. For the experiment, soapstone was obtained from two different quarries¹. One sample batch consisted of soapstone waste pieces, removed from a medieval church during restoration work, originally sourced from the local quarry at Rennesøy in Rogaland (Fig. 1). The other sample batch came from a modern soapstone quarry in Målselv, Northern Norway. Both types are light to medium grey when dry and dark grey when wet. The Rennesøy stone has a schistose structure and varies in hardness: some pieces are very soft and crumbly, easily scratched with a fingernail, while others are more solid. The Målselv soapstone is harder and has a more massive and homogenous structure. Both types have sporadic harder inclusions, probably of quartz and pyrite, varying from small nodules of ca. 1 mm in diameter to bands of several mm thickness which cut through the soapstone.

Four different grinding slabs were obtained to grind the soapstone pieces into desired shape, made of Devonian sandstone (1), red quartzite

¹ The materials were acquired by donation from the stone masons working with the restoration of St. Swithun's Cathedral, Stavanger.



Fig. 3. EPO examined in this study (photo: Simon Radchenko/Anja Mansrud).

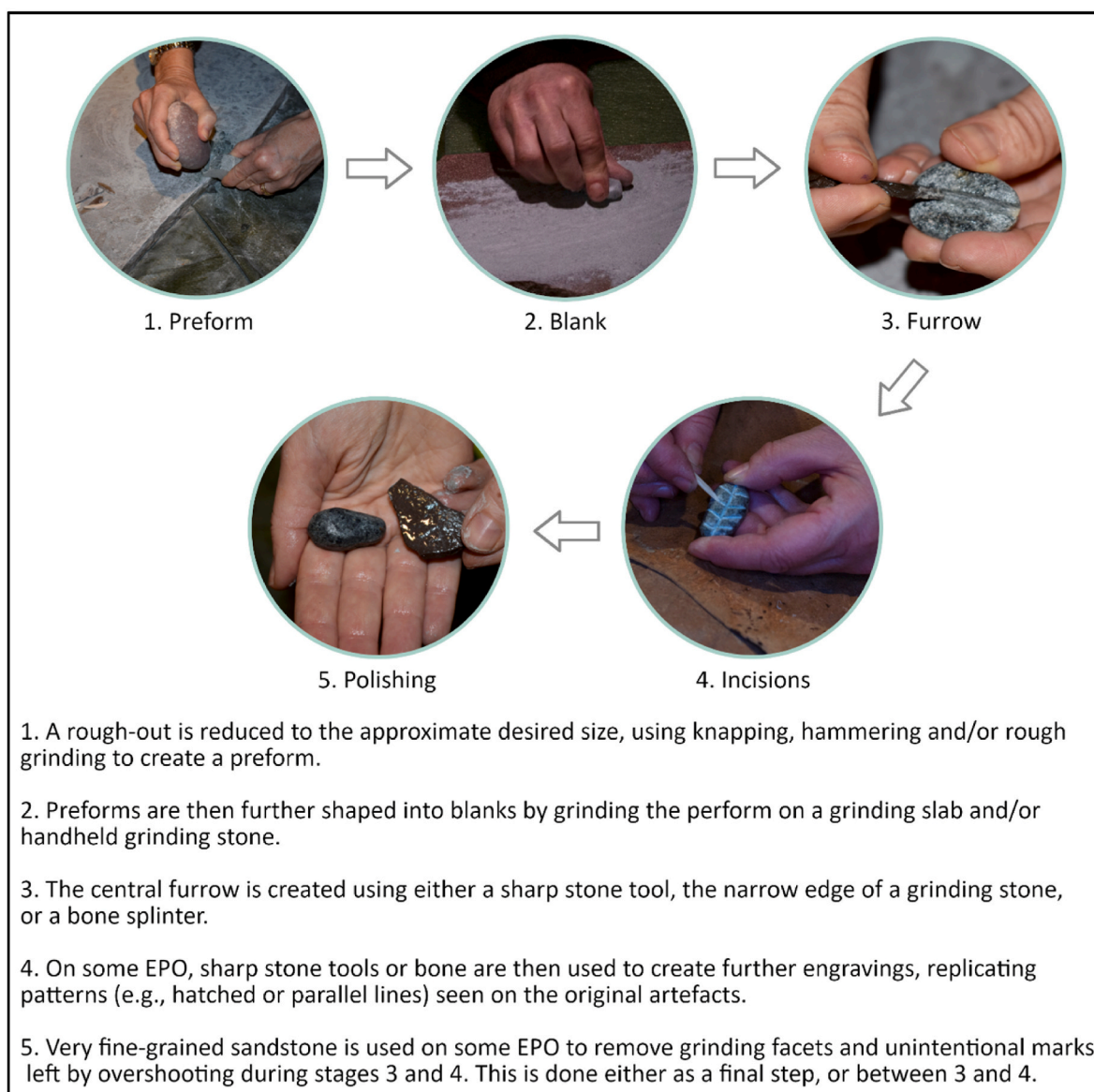


Fig. 4. Outline of the main production sequence involved in EPO manufacture (figure: Mette Adegeest).

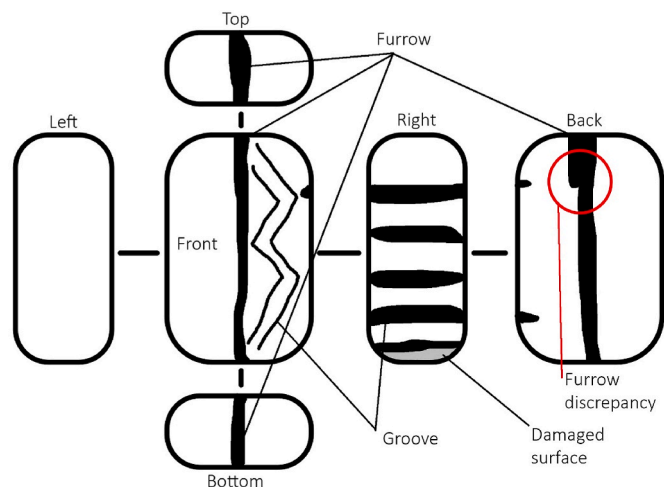


Fig. 5. Morphology and terminology of the features and surface modifications on bean sinkers used in this study (figure: Simon Radchenko).

(2) and quartzite slate (3, 4); along with four handheld grinding stones made of Ringerike sandstone (5) and red sandstone (6, 7, 8). Altogether the grinding stones range in texture from very rough and uneven to on par with rough sandpaper. This pilot study focuses on sinkers from Rogaland, South-Western Norway. During the late Mesolithic and early Neolithic period, the lithic tool-inventory in this region is dominated by blade-industries, produced from flint, mainly from small pebbles collected from beach moraine deposits. Quartz, rock crystal and quartzite was to a lesser degree utilised for manufacturing blades and microblades (Solheim, 2007; Meling et al., 2020; Nyland, 2016). These lithic raw materials were thus assumed to be likely candidates for working soapstone artefacts and were subsequently selected as working tools in the experimental replication of sinkers. In addition, we wanted to investigate whether soft soapstone could also be modified using bones. Flint blades were produced by indirect percussion and flint microblades by pressure technique; flakes of rough quartz were knapped using direct percussion; and bone splinters were produced by crushing bone with a hammerstone. For this initial experiment we opted for a limited number of raw materials which allowed us to reduce the number of variables. While few in number, tool materials chosen represented relatively diverse options: rough flaked stone (quartz), fine flaked stone (flint), blunt coarse stone tools (grinding stones) and bone. Other types



Fig. 6. a — EPO25, and b — EPO28, with the tools used to make the furrows. I — a bone splinter; II — thin sandstone grinding stones; III — flakes of rough quartz; IV — a flint microblade (photo and illustration: Simon Radchenko and Mette Adegeest).

Table 2

Metric, visual, and calculated parameters of 3D models under study.

No	Resolution (triangle size), microns	Alignment error (control scale bars), microns	Accuracy (calculated), microns	Accuracy (based on resolution), microns	Model volume, mm ³	Sinker density, kg/m ³
Experimentally produced objects						
EPO7	56	20	6	168	2931.5	2851
EPO8	59	11	40	177	3338.8	3339
EPO25	50	5	8	150	–	–
front						
EPO25	37	16	44	111	–	–
back						
EPO28	37	44	44	111	–	–
Archaeological artefacts						
S10358.e	42	20	59	126	5104.3	3590
S9360t	72	3	11	216	1874.5	3550
S9604	61	57	265	183	3491.4	3036
1930						
S10358.z	57	6	6	171	3567.5	3659s
S13484.11	58	6	11	174	4926.4	3462

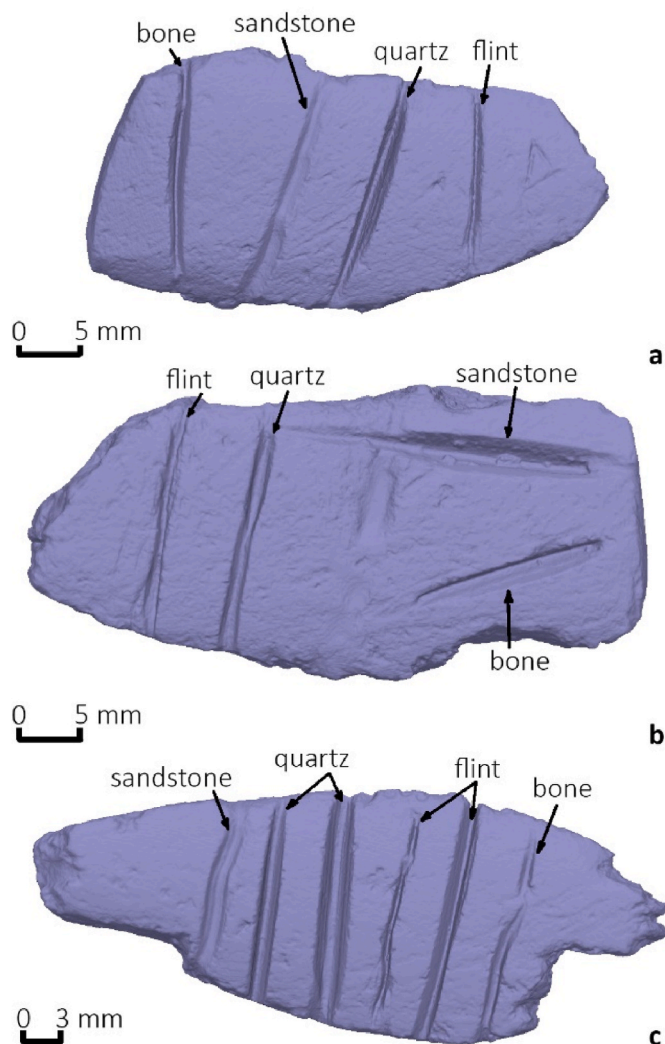


Fig. 7. 3D models of the experimental reference surfaces and grooves with the production tool indicated. a — EPO25 bottom side; b — EPO25 top side; c — EPO28 only one side was worked (Illustration: Simon Radchenko).

of lithic raw material such as mylonite, rock crystal and fine-grained quartzite were also used in Mesolithic Western Norway (Bjerck, 2010, Nyland, 2016) and should be tested in future experiments.

A total of twenty-six replicas were produced (Fig. 3). Drawing on observations of the archaeological specimens and prehistoric technological methods, basic blanks were manufactured. Additional manufacturing techniques and tools were tested to gain experiential knowledge of the workability of raw material and techniques, and to acquire a diverse range of examples for the digital imaging reference collection. Throughout the manufacturing sessions experimentally produced objects (EPO) were compared with 3D models of archaeological sinkers. These comparisons further guided our choices as we worked towards finding suitable combinations of tools and techniques that would most accurately replicate the originals. The general production sequence is outlined in Fig. 4; for a glossary of terms used in this paper, see Fig. 5 and Supplement A.²

A variety of techniques were tested in making replicas, including 1) short, repeated strokes to form lines; 2) long, uninterrupted strokes; 3) carving unidirectional lines; 4) carving bidirectional lines; 5) grooving

with the long edge of a sharp stone tool; 6) grinding and 7) both wet and dry carving and grinding. In addition to crafting replicas, two test pieces were created (EPO25 and EPO28) to form the basis for 3D-modelling (Fig. 6). Before engraving, the surfaces were ground into a slightly convex profile, but the pieces were not extensively shaped. Whilst acknowledging that not all variables can be controlled in an actualistic experiment like this, we attempted to create test pieces where differences between furrows would more likely be the result of variation in the tool material or technique, rather than variation in soapstone hardness/texture or differential forces applied by different makers. Hence, several furrows were made by the same person, using different tools and techniques but the same amount of time, and aiming to apply the same force and angle. Ninety seconds were used per furrow; sufficient time to produce a furrow of serviceable depth but short enough for the crafter to work continuously without hand and arm muscles tiring, which would affect the amount of force and precision. To ensure the possibility of replicating the experiment, the working processes were extensively documented by film and photo.

EPO25 (Fig. 6a) enabled comparison between wet and dry carving as well as different tool materials (a flint microblade, a quartz flake, a thin sandstone grinding stone and a bone point), with four furrows on either side made by four different tools, wet on one side and dry on the other. For each tool, the same technique was employed to either side. On the dry side no problems were encountered; on the wet side quartz inclusions made it difficult to carve into the soapstone which affected the shape of the created furrows. EPO28 (Fig. 6b) allowed a comparison of mainly different tool materials, and additionally to compare carving with the point to sawing with the long edge using a quartz flake and a flint microblade. All grooves were made on the same side of a piece of soapstone, selected for its relatively high homogeneity and a visual lack of quartz inclusions. As with EPO25, a bone point and a thin piece of sandstone were used in addition to the quartz flake and flint microblade. A third test piece, EPO8, was ground into an oval shape. Furrows were then made by means of a flint microblade, a quartz flake and thin piece of sandstone. No bone furrow was created on this piece. Stone tools were employed using a sawing motion to create the three furrows.

2.2. Image-based 3D modelling

The details on the data acquisition, including nuances of the toolkit, adjustments that were made to reach the high resolution and the sub-millimeter accuracy of the model, camera calibration parameters, mesh reconstruction parameters, and RSME values for the image-based 3D modelling, are outlined in the Supplement B. Data on resolution and accuracy evaluation are presented in Table 2. Based on this data, the results of our analyses are metrically reliable down to the scale of 0.2 mm (except for S9604, where the accuracy is 0.25 mm) and are visually reliable down to the scale of 0.06–0.07 mm. The software's margin of error for linear measurements depends on the alignment of each particular dataset and varies between 12 and 118 μm for different models under study (two times the accuracy calculated using Agisoft Metashape check scale bars measurements, see Table 2), while the margin of error with regards to the resolution of the model varies within 240 and 530 μm . Results with even higher precision and accuracy can be achieved with more elaborate equipment.

2.3. Digital study of engraved soapstone surfaces

Lately, promising results have been obtained with photogrammetry and laser scanning, including the detection of poorly visible traces (Arca, 1999; Güth, 2012; Domingo et al., 2013; Carrero-Pazos et al., 2018), relative chronology (Mélard, 2010; Mélard et al., 2016; Milner et al., 2016; Rondini, 2018; Radchenko and Nykonen, 2019; Radchenko et al., 2020; Galantucci et al., 2020) and nuances of production technology (Hermon et al., 2018). With the further development of 3D modelling protocols (Marín-Buzón et al., 2021; Cerasoni et al., 2022),

² 3D models used in the study are available at the link <https://doi.org/10.5281/zenodo.11528043>.

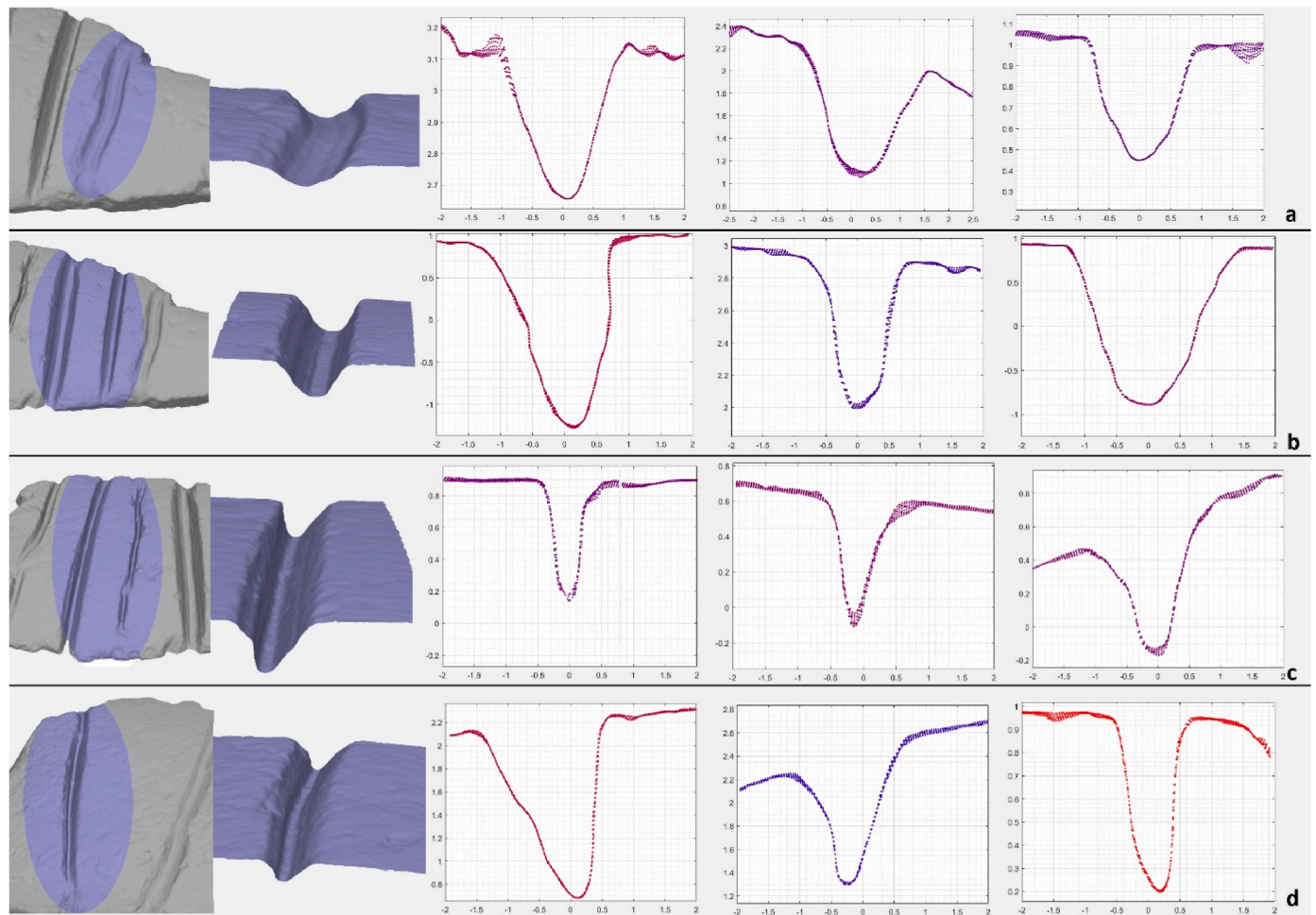


Fig. 8. Cross sections of the experimental engravings. a — made with sandstone; b — made with quartz; c — made with flint; d — made with bone. Scale in mm. (Illustration: Simon Radchenko).

Table 3
Quantitative parameters of engravings on EPOs under study.

		Number of slices	Average Depth, mm	Average depth variation from average, mm	FWHM, mm	Depth/FWHM ratio	MP count	Frequency of MP changes per mm
EPO25	Bone 1	25	1211	0,094	0,780	1,55	1,88	0,32
	Bone 2	15	1472	0,057	1038	1,42	2,40	0,53
	Flint 1, Blade	18	0,809	0,042	0,776	1,04	2,00	1,07
	Flint 2, Microblade	21	0,735	0,006	0,515	1,43	1,05	0,36
	Quartz 1	30	2117	0,083	1185	1,79	3,11	1,48
	Quartz 2	22	1050	0,069	0,896	1,17	2,50	1,00
EPO28	Sandstone 1	18	0,482	0,017	1203	0,40	2,06	0,44
	Sandstone 2	11	1116	0,060	1501	0,74	1,55	1,45
	Bone 3	16	0,830	0,012	0,699	1,19	2,00	0,00
	Flint 3, blade edge	26	1250	0,031	0,774	1,62	1,04	0,31
EPO8	Flint 4, blade point	19	0,925	-0,010	0,399	2,32	1,11	0,84
	Quartz 3, point	26	1565	0,067	1066	1,47	3,81	1,48
	Quartz 4, edge	27	1827	-0,014	1571	1,16	5,33	1,19
	Sandstone	19	0,619	0,032	1213	0,51	3,26	0,42
	Flint	24	1763	0,142	0,850	2,08	2,83	1,17
EPO7	Quartz	22	1629	0,165	1744	0,93	4,09	1,64
	Sandstone	20	1094	0,003	1413	0,77	3,50	1,20
	Quartz furrow 1	19	1,51	0,01	1,01	1,49	4,11	1,68
EPO7	Quartz furrow 2	19	1,49	0,03	1,03	1,45	3,53	1,89
	Microblade 1	7	0,36	0,02	0,36	0,99	1,00	0,00
	Microblade 2	9	0,42	0,04	0,60	0,70	1,00	0,00

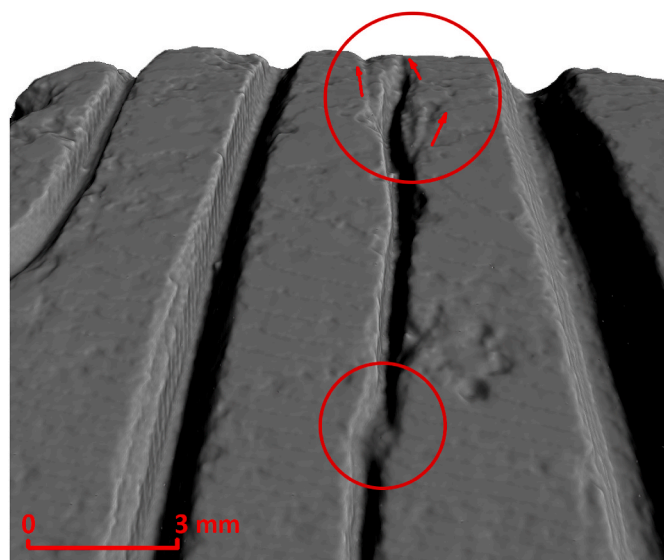


Fig. 9. Engravings made with flint by sawing (left) and carving with the flint point (right). A circle indicates areas of interest — quartz inclusions that were difficult to carve (below) and random fluctuations of the tool movements “overshoots” (above) caused by the carver’s lack of control when using the flint’s distal point compared to sawing with the flint’s long lateral edge (Illustration: Simon Radchenko).

the study of production techniques has been expanded paying additional attention to the cross-sections of engraved surfaces and their metric parameters (Haaland et al., 2021; Radchenko and Kiosak, 2022; Dubinsky, David & Grosman 2023; Płonka et al., 2023; Radchenko, 2023). While all these studies provide valuable insights into surface modifications of prehistoric artefacts, interpretations should be enhanced by experimentally retrieved information (as discussed in Radchenko, 2023; Płonka et al., 2023).

Here, the digital study of the archaeological sinkers and

experimentally produced objects consisted of four main stages, with workflow composition varying depending on the specific surface:

- 1) Visual examination and metric measurement of the objects and related engravings in Agisoft Metashape; volume and density calculations. Density is calculated as weight divided by the 3D model volume. The embedded Metashape formulas automatically calculate the latter.
- 2) Visual examination of the models (imported as *.obj) via Meshlab software, performed with the Radiance Scaling Shader and Ambient Occlusion filter. The examination utilised the artificial light source functions of Meshlab to benefit from the analysis of the surface position, orientation and the close reading of the stone’s relief.
- 3) Metric and visual study of engravings via the ArchCut_3D software solution (Dubinsky et al., 2023). Each engraving was represented by a four to 5-mm-long fragment (post-processing parameters are provided in Table 2). Metric and visual data were saved and examined separately. They are discussed in detail in the further sections. Data was imported as upscaled (scaled 1000:1 to fit the software requirements) models and transformed to *.wrl format.

For ArchCut_3D, we followed the methodology outlined in (Dubinsky et al., 2023), adjusting it to the specifics of a dataset and considering the accuracy limitations. For a series of cross-sections with an interval of 0.25 mm, we extracted their depth and FWHM (full width at half maximum depth). The average for both parameters and the ratio of Depth to FWHM were then calculated. Minimum points (MP, or minimum extremum points — spots on the cross-section graph, where the cross-section line visibly changes direction, signifying the complication of its geometry) were calculated for each engraving and reconfigured to reveal the frequency of MP change per 1 mm. These parameters were extracted for each series of slices and compared between different engravings: first experimental, then the artefacts.

- 4) In cases where the engraving’s superimpositions were a matter of interest, the Topography Visualization Toolbox (Horn et al., 2019;

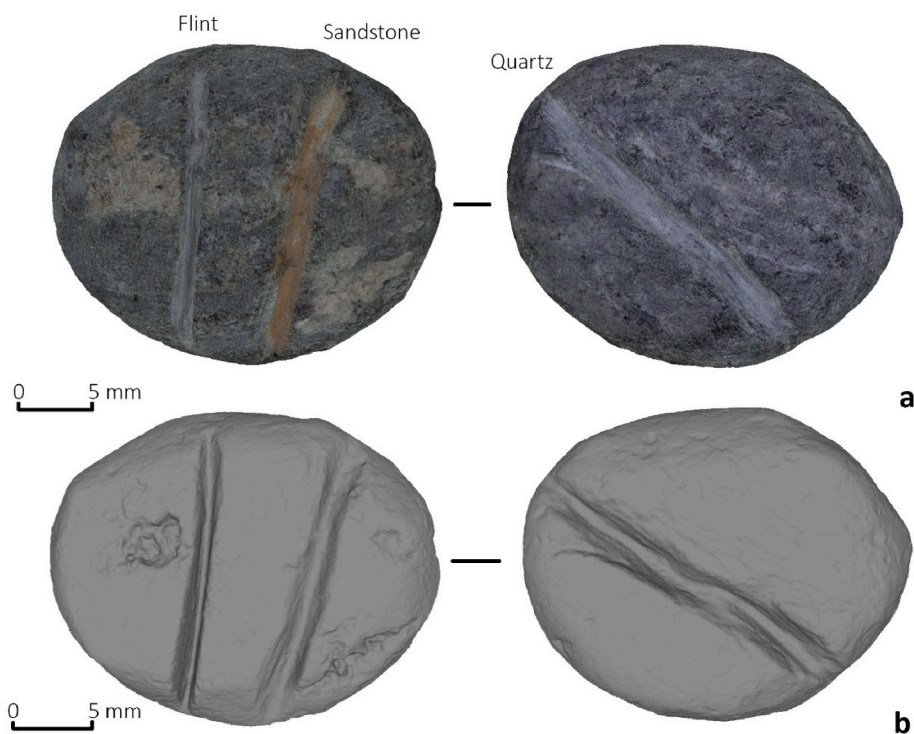


Fig. 10. 3D model of EPO8 with engraving tools marked. a — textured 3D model; b — 3D mesh (Illustration: Simon Radchenko).

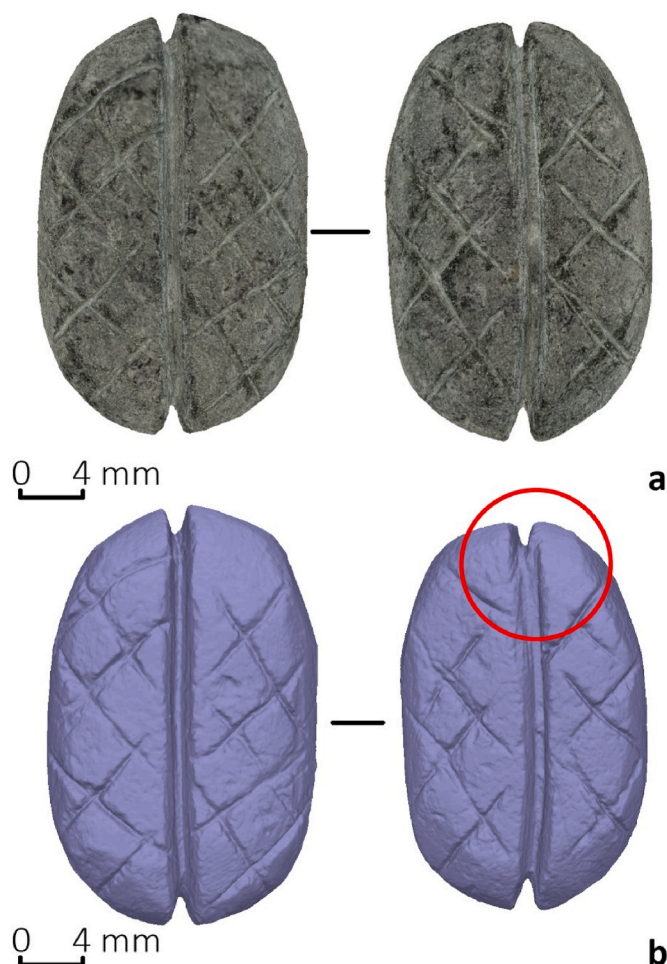


Fig. 11. Front (left) and back (right) sides of the 3D model of EPO7. a — textured model; b — 3D mesh. The circle indicates the final point of the furrow production on the back side of a sinker (Illustration: Simon Radchenko).

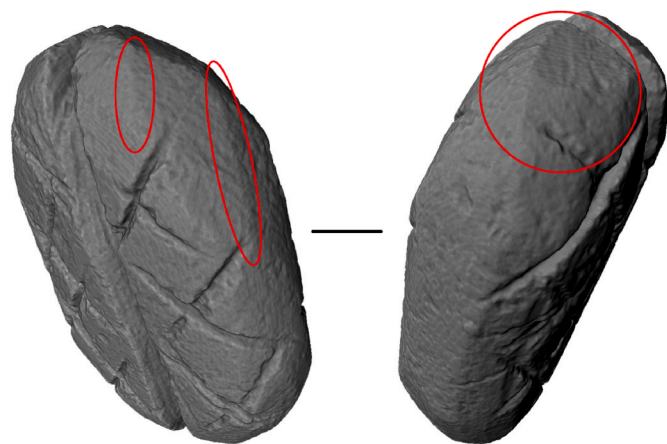


Fig. 12. 3D mesh of the EPO7. Circles point to the edges of grinding facets (Illustration: Simon Radchenko).

Horn et al., 2022) was utilised as a highlight tool, enabling a closer look at the geometry of the intersections of the lines (a methodology tested in Radchenko et al., 2020; Radchenko and Kiosak, 2022).

The digital study resulted in a detailed report on characteristic features, possible engraving sequences, and fragments of personal

biographies of each modelled artefact. The conclusions based on experimentally produced objects were subsequently calibrated with the data from actualistic experiments, while the conclusions regarding the archaeological artefacts were eventually compared to the experimental data. This comparison utilised image-based 3D modelling as a bridging method to make the close analysis of two different datasets possible. To our knowledge, no comparable studies, analysing engravings in soapstone or similar soft stone materials by means of 3D-modelling, have so far been conducted. To validate the results, this novel approach should be replicated in future studies.

3. Results

3.1. Digital study of the experimental datasets

Image-based 3D modelling of EPO25 and EPO28 was used as a reference point for determining characteristic features of the engraving process undertaken with tools made from different materials. The engravings, with production time controlled, made on a ground surface, formed the basis for cross-section extraction and further analysis (Fig. 7).

Results show that different tools clearly produce visually different negatives on a soapstone surface (Fig. 8). As soapstone is a soft material, the shape of the negative is related to the morphological shape of each individual tool employed and is not necessarily linked to the geology of the lithic engraving tools. Visual differences between the variously made engravings and their quantificational representation (see Table 3) do not provide 100 % reliability, but does reveal possible options.

Engravings made with sandstone (Fig. 8a) were the easiest to distinguish - the imprints are shallower and wider than imprints left by the other tools. Red sandstone tools also coloured the negative imprint reddish, which may or may not be detectable archaeologically. The Depth/FWHM ratio is significantly lower than in other cases and remains beyond 0.8. MP count and frequency of changes vary for different engravings, which generally indicates the strong influence of other factors, such as irregularities and inclusions into the engraved surface. This contrasts with the quartz marks, which have a Depth/FWHM ratio of 1 or higher. The distinctive feature of the quartz-made marks is a high MP number (consistently above 2, sometimes 3 or 4) that presents cross-sections as having complex irregular shapes made by a hard angular tool. This number changes with an average frequency of 1–1.5 times per mm, the highest among the four different engraving materials tested; meaning that imprints made with quartz tools are very different depending on the relative positioning of the tool in the groove.

Flint-made engravings (Fig. 8c) are different from those from quartz (Fig. 8b) by several parameters. Not only is their Depth/FWHM ratio slightly higher (sometimes hitting two or more), the MP count is also relatively low and rarely exceeds 2. Moreover, the frequency of MP change per mm is significantly lower than that of quartz: between 0.5 and 1.5. These parameters reflect the fact that flint tools are usually thinner and sharper than quartz ones. From our experimental programme we observed that flint blades can cut through quartz or pyrite inclusions in soapstone, unlike other materials. It is, in theory, possible that a very thick flint blade produces an imprint morphologically like one made from quartz (or vice versa), but these cases are expected to be statistically minor. It is worth noting that the cross-sections produced by engraving with the point of a microblade/bladelet (in a burin-like fashion) are similar to marks made by the longitudinal flint edge in a sawing motion. Both having relatively high Depth/FWHM ratio (2.32), these negatives are almost indistinguishable by shape. Acquired experiential knowledge informs us that engraving with the point is less controllable than sawing, resulting in overshoot marks on the soapstone surface (see Fig. 9).

Engravings made with bone (Fig. 8d) share all their main features with flint—their Depth/FWHM ratio is between 1 and 1.5, and the MP number is relatively low and varies between 1 and 3. Noticeably, the

Table 4
Quantitative parameters of the engraved lines on the sinkers under study.

Artefact nr.	Engraving	Number of slices	Average Depth, mm	FWHM, mm	Depth/FWHM ratio	MP count	Frequency of MP changes per mm
S10358.e	Furrow back	22	1,897905006	1,453915397	1,305375134	2,545454545	1,090909091
	Engraving 1	12	1651	1009	1,64	1,42	0,67
	Engraving 2	11	1,264425936	0,977410852	1,29364835	2,384615385	1,230769231
S10358.z	Furrow back	23	1,076002527	0,905564875	1,18821142	2,043478261	0,869565217
	Furrow front	32	0,645995909	1,135035328	0,569141676	1,71875	0,75
S13484.11	Furrow back	25	0,904473234	1,437217107	0,63	1,64	0,96
	Furrow front	27	0,926917316	1,422453195	0,651632911	2,777777778	0,888888889
S9360t	Furrow front	27	0,47664964	0,702687283	0,678323988	1	0
	Furrow back	25	0,910	1375	0,66	2,40	0,16
	Engraving 1	14	0,286615038	0,681567261	0,420523483	1	0
S9604	Engraving 2	13	0,293424663	0,506750391	0,579031942	1	0
	Furrow back	11	1,910439193	1,217266872	1,569449755	2	1,090909091
	Furrow back 2	9	1,991889575	1,2543933	1,587930656	2,555555556	0,111111111
	Furrow front	10	1,405093993	1,407836986	0,998051626	3,5	0,8
	Furrow front 2	11	1,262744233	1,094269813	1,153960584	2,090909091	0,363636364
	Engraving 1	9	0,536052406	0,869652923	0,616398096	1,833333333	0,333333333
	Engraving 2	12	0,835406342	0,664395873	1,257392432	1,333333333	0,470588235
	Engraving 3	16	0,721609061	0,634274202	1,137692592	1	0
Engraving 4	12	0,941304994	0,81567503	1,154019628	1,888888889	0,444444444	

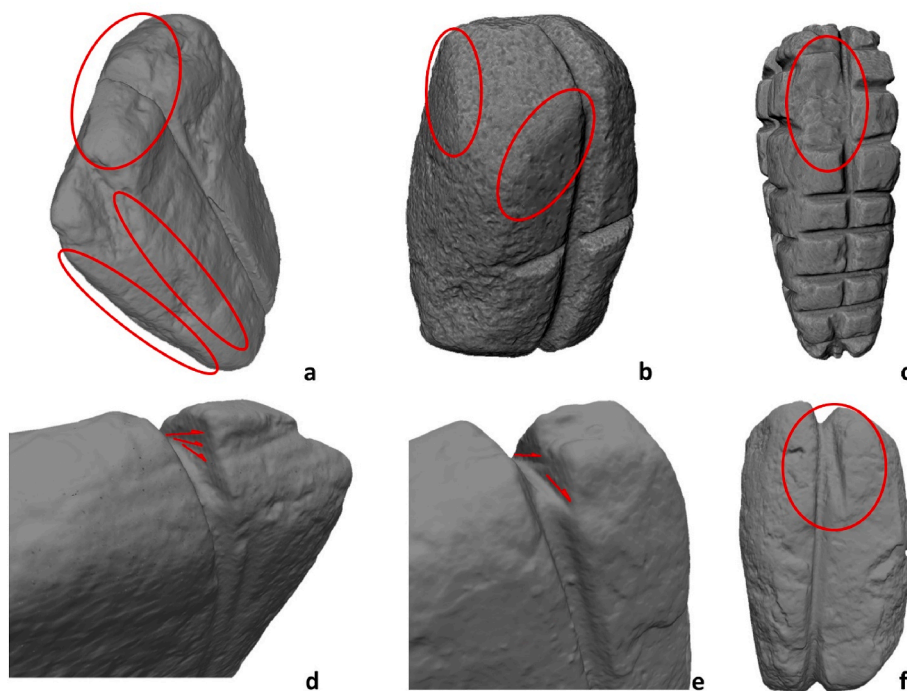


Fig. 13. 3D-mesh of the archaeological sinkers studied with the emphasised areas of interest. a, d, e — S10358.z; b, f — S13484.11; c — S9604. a, b — circles mark possible traces of grinding to shape the blank; c — circle marks the damage of the soapstone surface after engraving; d, e — arrows mark the tool inclination while engraving the narrow parts of the furrow; f — circle marks the discrepancy between the first and the last furrow engraving actions (Illustration: Simon Radchenko).

shape and softness of bone tools causes a significantly lower frequency of the MP variation — in all cases, it is below 0.55. This reflects the smoothness of bone surfaces and the small number of angular surfaces (compared to flint or quartz). These results were double-checked with the engravings of the EPO8 (Fig. 10), which were produced with different tools on the ground surface, with no controllable time. The cross-check revealed the same pattern for all three engravings: sandstone has the lowest Depth/FWHM ratio of 0.77, the quartz tool produced a groove with a high MP number (4.09), while sawing with a flint blade resulted in a fine and narrow engraving (Depth/FWHM ratio of 2.08) with a low number of both MP points (2.83) and the frequency of its change (1.17).

Importantly, 3D modelling of the EPO7 provided a digital reference for the future study of the 3D models of archaeological artefacts. This

experimentally produced object has been designed to replicate the main features of what can be generalised as a “standard bean sinker” (Fig. 5). It introduces the geometric configuration of a quartz furrow and the ornamentation made with a flint microblade. The digital study indicated the direction of furrow production and highlighted the traces of sawing the furrow with a quartz blade. This helped us distinguish between the “front” side of the sinker (where the furrow engraving was initiated) from the “back” side (where the engraving ends) (Fig. 11). A closer look at the sinker profile further revealed several traces of shaping the blank. From our experimental work we observed that if a soapstone sinker’s surface has flatness and observable edges between flat facets, grinding may have been used to shape the blank, though other possibilities should be explored via further experiments (Fig. 12).

The quantitative study of the cross-section parameters followed the

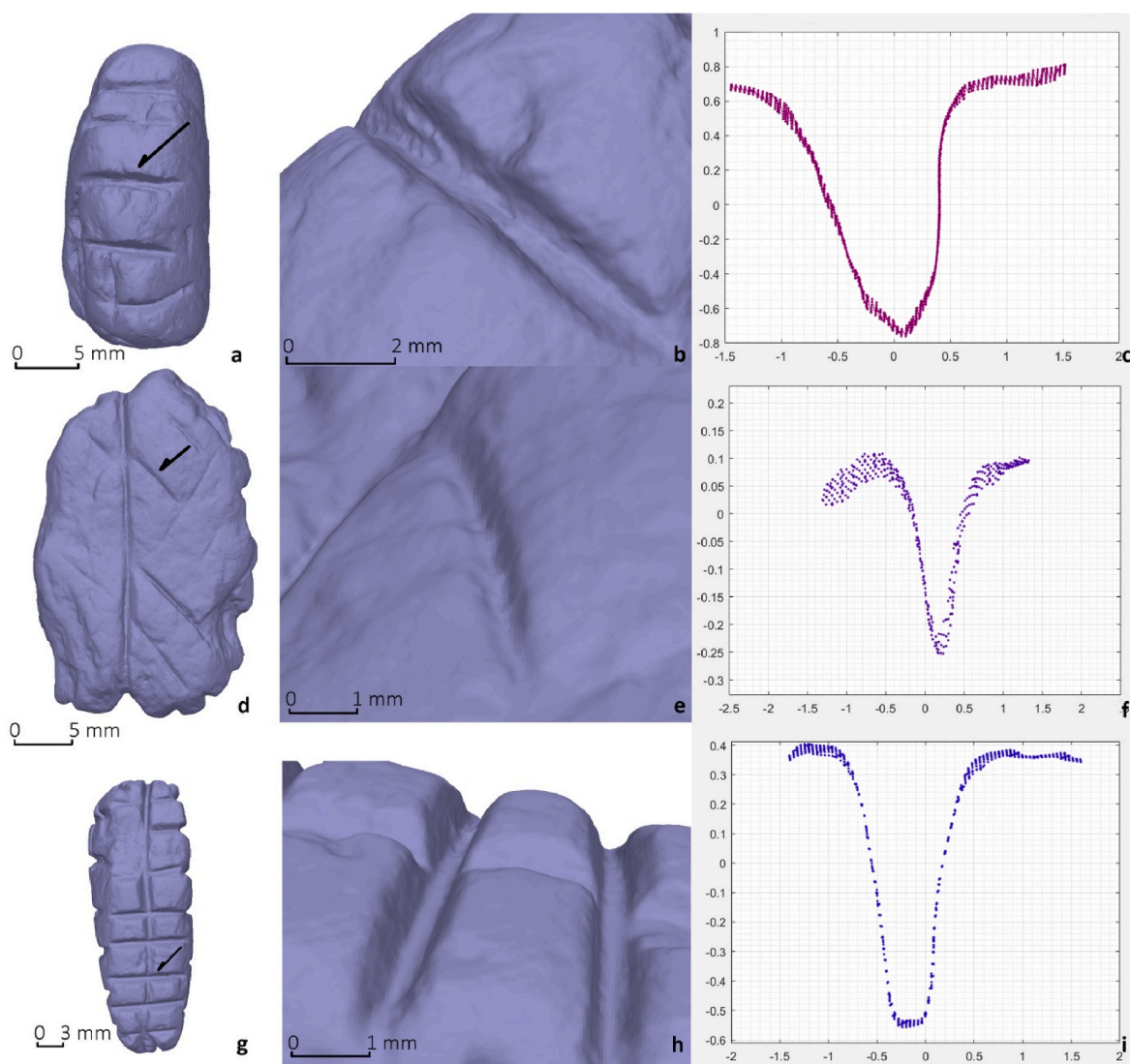


Fig. 14. Grooves on the surface of different sinkers under study. a–c — S10358; d–f — S9360; g–i — S9604. a, d, g — 3D-mesh of sinkers. Arrow points to grooves presented in close-up. b, e, h — a closer look at the grooves indicated by arrows; c, f, i — grooves in profile (scaled in mm) (Illustration: Simon Radchenko).

outlined pattern (see Table 3). Quartz furrow on the EPO7 is characterized by a high MP number (3.5–4), moderate frequency of MP variation (1.5–2), and a Depth/FWHM ratio of up to 1.5 — just as expected following the study of EPO25 and EPO28 with the reference engravings. The cross-hatched incisions made with a microblade returned the MP of 1 without any change, which is reasonable as these engravings are short and made with only several movements. Surprisingly, their Depth/FWHM ratio is low (<1) as the incisions are very shallow (all below 0.5 mm).

3.2. Digital study of the archaeological sinkers

Using the experimentally produced objects as a reference, we managed to interpret and explain features related to the production process of archaeological sinkers. All five of them were identified as representing the same type, though they vary in colour and incisions' arrangement. They are relatively identical metrically: 2.5–3.0 mm in length, 2.1–2.5 mm in width, and up to 1.4 mm in thickness. One specimen (S9360t) differs geologically. It is made from a layered slate rock and is significantly smaller than the others.

3D modelling provides an instrument for measuring the volume of modelled objects, enabling a means of measuring the sinkers' density

and thus, their “sinkability” — the parameter that defines their functional relationship with water. All five modelled objects have a total density of 3000–3650 kg/m³, implying they sink equally fast. This includes S9360t, which is considerably smaller and lighter than the others. What this suggests is that density, or ‘sinkability,’ is in fact a principal parameter for the sinkers, considered during the raw material selection and production phases.

Another key result obtained from the 3D modelling was that the soapstone surfaces appeared affected by erosion processes. Given the high level of surface erosion, we recommend that further studies of soapstone materials should consider the possibility that depositional and post-depositional processes may have caused considerable modification of the artefacts. Significantly, the condition of the surface directly affects the result of quantitative cross-section studies, with depth and width measurements possibly varying depending on the state of the surface (Table 4).

A closer look at the 3D models of the archaeological artefacts revealed several features pointing out different kinds of surface modifications. Some of them resemble traces of faceting that may indicate grinding a raw preform into a bean-shaped blank before making a furrow (Fig. 13a and b). Others show surface damage, enhanced by the engraving process, leading to sinker fracturing (see Fig. 13c).

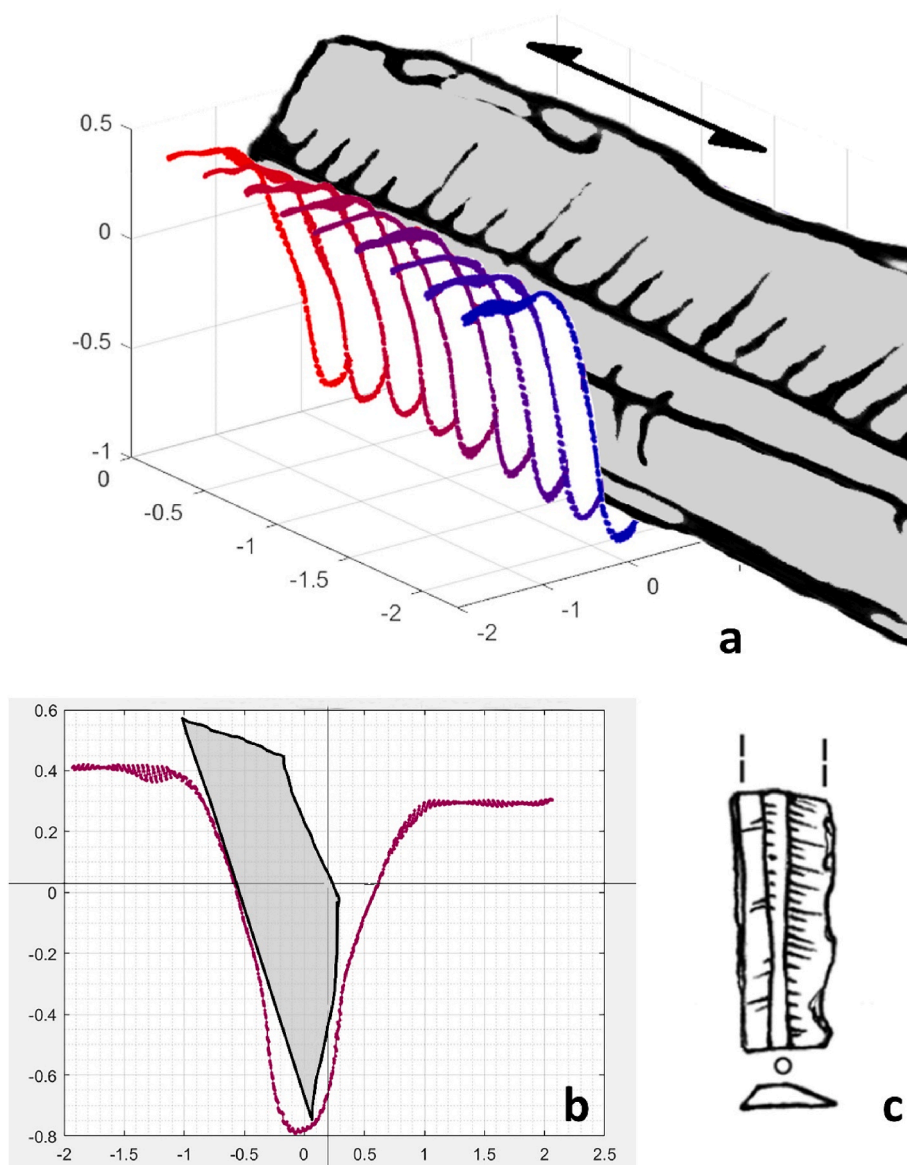


Fig. 15. Schematised image of the making of a “pear-shaped” cross-section with a narrow flint microblade. a — isometric view of the microblade entering the groove; b — the cross-section with the microblade profile marked in grey; c — drawing of a microblade. Scale is in mm. (Illustration: Simon Radchenko).

Studies of the engraved surfaces further provided insights into the details of the engraving process. For instance, a closer look at the furrow-making process allowed to determine the engraving direction on different facets of the studied artefacts. Leveraging experimentally acquired knowledge, digital observation revealed the sequence of specific engraving traces (Fig. 13d and e). Starting on the larger face, the engraving usually continues on the smaller (top and bottom) ones, moving further towards the ‘back’ side of the stone. Hence, it is often possible to tell the front side from the back one, as the latter exhibits a mismatch of the furrow line closer to the edges (Fig. 13f). Distinguishing these two sides allows for inferring the production sequence involved in making the furrow (see Figs. 5 and 17a for an illustrated example).

Quantitative analyses revealed the relative consistency of the furrow’s geometry. Even though archaeological objects are affected by surface erosion — the Depth/FWHM ratio is consistently lower at the more eroded surfaces — other parameters remain indicative. For all studied furrows, except those on the geologically different S9360t, the MP (minimum points) number remains relatively high (1.5–3.5 with an average of 2.3). This, together with the relatively low frequency of MP change per millimetre (0.1–1.1), points to *quartz as the most probable*

lithic tool used for producing the longitudinal furrow.

Grooves are yet another case (Fig. 14). Three out of five sinkers have grooves in addition to the central furrow. Noticeably, *these grooves are significantly different from the furrow* - visually and in calculations, even though morphologically, they may appear closer to those made with quartz tools (as in the case of S10358.e). Otherwise, crosshatches on the sinker S9360t are very shallow and wide (with a depth of around 0.3 mm and a Depth/FWHM ratio of around 0.4–0.6) — due to the geological variation of this type of stone — and have an MP of 1 without any variation. Altogether, these parameters suggest that incisions were made with a flint microblade. Finally, the grenade-shape sinker S9604 is incised with what can be interpreted as flint-made lines — Depth/FWHM ratio of 0.6–1.3, MP count of 1–2, and a low MP variation frequency per millimetre (0–0.5). These profiles are interesting due to their pear-shaped cross-section — evidence of a very thin engraving tool (Fig. 15).

This variation in engraved patterns, contrasted to the relative homogeneity of the longitudinal furrow production, underlines that the central furrow – assumed to be functionally related for fastening a line – was consistently made in a similar way on all the archaeological sinkers

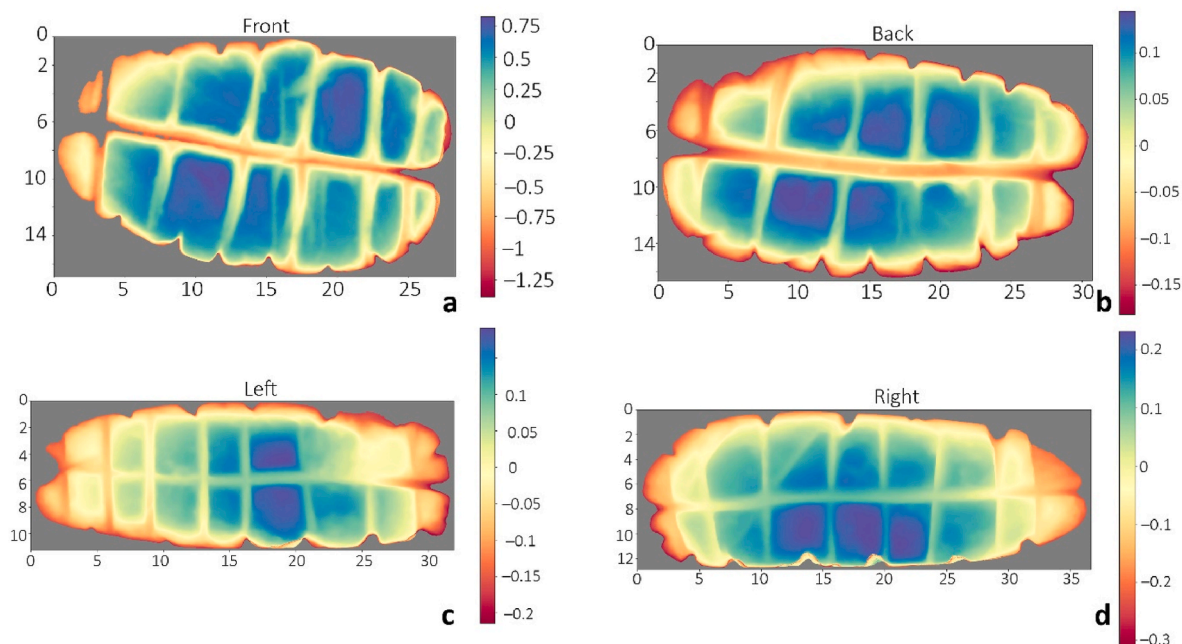


Fig. 16. Heatmap of S9604. The location of intersections between furrows and grooves indicates the relative chronology of the engraving process: a — front view; b — back view; c — left view; d — right view. Scale in mm. Produced with TVT. (Illustration: Simon Radchenko).

under study.

In addition, 3D modelling enabled the reconstruction of the relative chronology of the engravings, hence revealing the individual manufacture stages of each sinker. The number of grooves on the 3D model of sinker S9604 allows further detailing of how grooves interact with the furrow. As expected, the furrow was created first with the grooves perpendicular to the furrow superimposed. This is emphasised with a heatmap of surface relief, where the perpendicular grooves slightly slope towards the bottom of the furrow at the intersection points (see Fig. 16a and b). However, such effect is absent for the grooves on the left and right sides of the stone. On the contrary — the lines are straight, with almost uninterrupted perpendicular walls and exemplary cross-sections (see Fig. 16c and d). Moreover, there are no visible slopes at the grooves bottom in the places where they cross the furrow-like line on the left and right sides of the sinker. This indicates that the furrow crossing left and right side is the latest engraved addition to the sinker's surface. For both furrows, the engraving direction falls into the scheme described above (front — top — back — bottom — discrepancy at the back, where the furrow fails to close). At the second furrow, the engraving process started on the left side and went through the top towards the right one (Fig. 17). This sequence partially follows the pattern revealed through the experimental study but goes further, emphasising the relation between relatively homogeneous furrows and a variety of other marks on the soapstone surface.

4. Discussion

The excellent ability of 3D imaging techniques to reveal new information about the manufacture of archaeological artefacts is now well established; however, interpretations regarding surface modifications have thus far been limited to data obtained from 3D modelling of the artefact's surface. Integrating 3D modelling of experimentally produced objects (EPO) brought a new dimension to the research process: establishing a connection between the geometry of the archaeological surfaces, their characteristic features, and the production processes. Essentially, it enabled the creation of reference data that can be cross-compared with the originals, assisting interpretations relating to the manufacture process. Through comparison with experimental data,

previous assumptions concerning manufacture techniques and function can be verified or rejected using visual and quantitative studies. The present research thus provides new empirically grounded evidence which supports prior theories that proposed the use of flint and grinding tools in sinker manufacture and engraving (Bergsvik, 2017: 79, 86). While the choice of these materials/tools seems logical, based on their frequent occurrence in archaeological record, our integrated method has not only helped verify past assumptions, it provides new data showing that quartz played an important role as an engraving implement - used for making the central longitudinal furrow. Differences in production tools, we argue, only become “visible” via the detailed study of 3D-modelled surfaces, making it possible to distinguish flint-made surface modifications from quartz, bone, or sandstone. In sum, this integrated method reveals new empirical data about these key aspects of a sinker's biography:

1. Initial shaping of the blank using grinding stones
2. Engraving direction and the sequence of furrow production
3. Ability to identify and distinguish differences in the toolkit used for engraving
4. Relative chronology of the engraving process
5. Damage to the artefact surface caused during use-life and via post-deposition processes

This study has been able to demonstrate that the central furrow was produced in a consistent way, likely with quartz tools, while other incisions showed more variation. Aesthetic concerns are one possible reason for this difference, though others should be considered; future studies may help provide greater insight into the reasons driving this preference. It should, however, be remembered that a larger dataset of analysed bean sinker artefacts may expose new/different patterns.

Nonetheless, our results have allowed the first insights into the operational sequences of soapstone sinker manufacture, thanks to digital and quantitative experimental evidence. Whilst we stress that a much larger analytical study of archaeological sinkers from different sites/regions is needed to identify potential variation (spatially and/or temporally) in the mode of production, our study enables a broad outline of the main steps and toolkit. This involves making a preform by

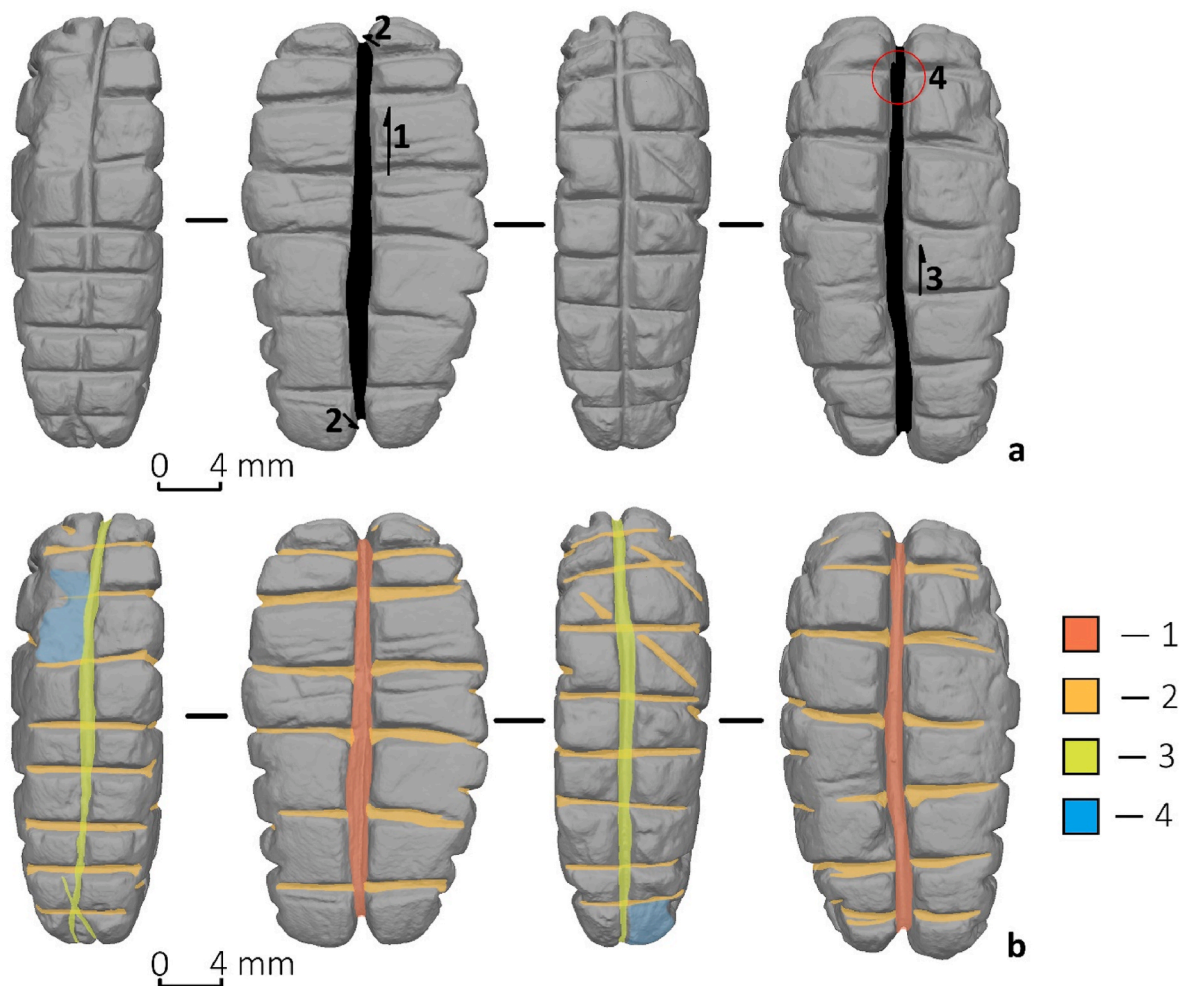


Fig. 17. Chronological sequence showing the phases of engraving sinker S9604. a — The first phase is the engraving of the furrow. Black arrows point to the sequence and direction of furrow production. b — Relative chronology of the remaining engraving process. 1/red: Engraving the central furrow production; 2/orange: making the grooves on the central surface, 3/green: making the furrow on the left and right side; 4/blue: indicating areas with erosion (PDSM). (Illustration: Simon Radchenko). (For interpretation of the references to colour in this figure legend, the reader is referred to the web version of this article.)

knapping or grinding a soapstone piece into roughly the required shape and size. Since this is a reductive technique, producing powder or small irregular soapstone pieces, these are not likely to be picked up during excavation and unworked or only roughly shaped preforms or blanks would not necessarily be recognised as artefacts. Some surface modifications interpreted as grinding traces are observable via the photogrammetric study. Image-based 3D modelling also indicates that the central furrow was most likely made with a quartz flake, while grooves that post-date the central furrow and are likely made with other tools, likely made of flint. They are relatively later additions, probably made ad-hoc, given the variation in patterns and the tools and techniques employed.

Combining experimental research with photogrammetry has revealed a hidden potential in joint use of both methods. To begin with, a photogrammetric study — from the simple 3D model observation to the high-level computational analyses — enables a closer look at the morphology and configuration of the furrow and grooves. Each studied artefact revealed a micro-piece of evidence regarding the common elements and the unique features of their biographies. Given the scalability of photogrammetry, the application of this method is only limited to our ability to interpret the information provided by the 3D model surface. Experimental archaeology brings an additional dimension to that process by supplying new information on how the surface configuration is related to the specific engraving process, direction, production or

deposition damage. Thus, it bridges the gap between the data extracted from photogrammetry and their technological interpretation.

Conversely, studying the 3D models during the actualistic experimental replication sessions meant we were able to take a more flexible/responsive approach, testing theories as new information emerged. For example, EPO25 and EPO28 (engraved with various tools over controlled time) were produced following the preliminary photogrammetric results with EPO7 and EPO8 (made to replicate the soapstone sinkers). Therefore, a comparable dataset for the digital study has been made upon reflection on the first round of experiments and digital modelling. On the other hand, the actualistic experiments happened to provide good reasoning for selecting the engraved surfaces for the detailed digital study more consciously. In this way, the application and integration of 3D digital and experimental archaeology enabled genuinely interdisciplinary communication, a result difficult to obtain but when achieved, often comes with blue sky potential. In sum, working reflexively between photogrammetry and experimental archaeology was an important source of new ideas in both directions.

5. Conclusions

Recent advances in image-based 3D modelling techniques have expanded the potential of photogrammetry to the analysis of engraved portable stone artefacts (e.g., [Mélard et al., 2016](#); [Haaland et al., 2021](#)).

While confocal microscopy and tomography promises higher resolution of the model, photogrammetry remains advantageous in terms of the affordability, scalability and portability of the modelling tools. However, the reliability of 3D modelling results is grounded in the accuracy control and assessment solutions during the photogrammetric data acquisition stage. Since most technological studies rely on the microscopic features of the studied surface, they often depend on specific methodological approach. By looking at the submillimetre details beyond the suggested accuracy of many laser scanning devices, this study emphasises the matter: the only way to provide reliable technological conclusions on that scale is by avoiding black boxes and being aware of how research tools produce the data.

Applied this way, photogrammetry can reveal numerous technological features of ancient crafting and artmaking practices, especially when combined with experimental studies. For the soapstone sinkers from Western Norway, it significantly increased the knowledge on the biography of the artefacts — from making the blank to the erosion and taphonomic processes, highlighting features otherwise invisible or unnoticeable. Whilst not providing decisive answers to all the technological questions, detailed analysis of soapstone sinker replica and artefact surfaces enabled us to distinguish between shapes made with various tools. Though not able to identify the engraving tools with 100 % certainty, the experimental and digital pilot study enabled us to determine the most probable options. Future research expanding the corpus of archaeological sinkers is currently under way, as it is recognised that the dataset discussed here is limited, with a larger quantity opening potential for greater variation in the method of manufacture.

Irrespective of sample size, this interdisciplinary combination of photogrammetry and experimental archaeology has proven to be a very efficient way of tracing the connections between specific technological procedures and the surface configuration of archaeological artefacts. The tiniest details, observed on the experimentally produced objects by means of image-based 3D modelling served as markers of various engraving techniques. This allowed extrapolation to archaeological artefacts and nuanced our knowledge of the techniques and tools involved in making them. Employing experimental archaeology and digital analysis simultaneously highlighted details that easily would have been overlooked by only using one of these methods. This integrated approach has great potential for further study of different kinds of engraved surfaces, including portable art objects, made from stone and other types of materials.

CRedit authorship contribution statement

Simon Radchenko: Writing – original draft, Visualization, Software, Methodology, Investigation, Formal analysis, Data curation. **Mette Adegeest:** Writing – original draft, Visualization, Methodology, Data curation. **Aimée Little:** Writing – review & editing, Validation, Supervision. **Anja Mansrud:** Writing – review & editing, Validation, Supervision, Resources, Project administration, Funding acquisition, Conceptualization. **Morten Kutschera:** Formal analysis, Data curation.

Declaration of competing interest

The authors declare that they have no known competing financial interests or personal relationships that could have appeared to influence the work reported in this paper.

Acknowledgements

The authors would like to thank the stone masons, in particular Ann Kathrine Meeks, at the St. Swithun's Cathedral for providing access to soapstone and Agder Fylkeskommune for lending us an excellent workspace to carry out the experiments at Lista in January 2024. The research was made possible by the kind support of the Scholars at Risk network. It was partially funded by the European Union's Horizon

Europe train and mobility actions programme under the Marie Skłodowska-Curie grant agreement No. 101153375.

Appendix A. Supplementary data

Supplementary data to this article can be found online at <https://doi.org/10.1016/j.daach.2025.e00427>.

References

- Arca, A., 1999. Digital Auto-Tracing in Rock Art Recording: Applications of Computer Vectorial Designs, vol. 11. *Tracce Online Rock Art Bulletin*. <http://www.rupestre.net/tracce/traccell.html>.
- Åstveit, L.I., 2008. Mellommessolitisk tid (MM) 8000–6500 BC. In: Bjerck, H.B. (Ed.), *NTNU Vitenskapsmuseets Arkeologiske Undersøkelser Ormen Lange Nyhamna*. NTNU, pp. 571–574.
- Bakkevig, S., 2021. En liten klebersteinsgjenstand fra steinalderen på Bokn – del 2. *Frå haug ok heiðni* 2021 (1), 21–25.
- Bamforth, D.B., 2010. Conducting experimental research as a basis for microwear analysis. In: Ferguson, J.R. (Ed.), *Designing Experimental Research in Archaeology: Examining Technology through Production and Use*. University Press of Colorado, pp. 93–109.
- Bergsvik, K.A., 2017. Mesolithic soapstone line-sinkers in Western Norway: chronology, acquisition, distribution, function and decoration. In: Hansen, G., Storemyr, P. (Eds.), *Soapstone in the North: Quarries, Products and People. 7000 BC – AD 1700*. University of Bergen, pp. 73–92. <https://hdl.handle.net/1956/16580>.
- Bjerck, H.B., 2010. Norwegian Mesolithic trends: a review. In: Bailey, G., Spikins, P. (Eds.), *Mesolithic Europe*. Cambridge University Press, pp. 60–106.
- Björge, T., 1981. Flatøy – Et Eksempel På Steinalderens Kronologi Og Livbergingsmåte I Nordhordaland. Unpublished MA Thesis. University of Bergen.
- Bøe, J., 1925. Bergens museums tilvekt av oldsaker 1924. In: Kalderup, C.F. (Ed.), *Bergens Museums Årbok 1924-1925*. John Griegs Boktrykkeri, Bergen.
- Bøe, J., 1934. Boplassen i Skipshelleren på Straume i Hordaland. *Bergens Museums Skrifter* 17.
- Carlsson, T., 2007. Axe production and axe relations. In: Olausson, D., Jennbert, K., Hårdh, B. (Eds.), *On the Road: Studies in Honour of Lars Larsson*, pp. 157–160.
- Carrero-Pazos, M., Vilas-Estévez, B., Vázquez-Martínez, A., 2018. Digital imaging techniques for recording and analysing prehistoric rock art panels in Galicia (NW Iberia). *Digit. Appl. Archaeol. Cult. Herit.* 8, 35–45. <https://doi.org/10.1016/j.daach.2017.11.003>.
- Cerasoni, J.N., Nascimento Rodrigues, F., Tang, Y., Yuko Hallett, E., 2022. Do-It-Yourself digital archaeology: introduction and practical applications of photography and photogrammetry for the 2D and 3D representation of small objects and artefacts. *PLoS One* 17 (4), e0267168. <https://doi.org/10.1371/journal.pone.0267168>.
- Conneller, C., Little, A., Birchenall, J., 2018. Making space through stone. In: Milner, N., Conneller, C., Taylor, B. (Eds.), *Star Carr Volume 1: A Persistent Place in a Changing World*. White Rose University Press, York, pp. 157–221.
- Damlien, H., Nylund, A.J., Redmond, J.J., 2024. Lithic technology before and after the Storegga tsunami (8200 cal BP): dissolving large-scale regional trends to identify social impact of crisis in western Norway. *Holocene* 34 (12), 1790–1806. <https://doi.org/10.1177/09596836241274987>.
- Domingo, I., Villaverde, V., Lopez-Montalvo, E., Lerma, J.L., Cabrelles, M., 2013. Latest developments in rock art recording: towards an integral documentation of Levantine rock art sites combining 2D and 3D recording techniques. *J. Archaeol. Sci.* 40, 1879–1889. <https://doi.org/10.1016/j.jas.2012.11.024>.
- Dubinsky, L., David, M., Grosman, L., 2023. Recognizing technique variation in rock engravings: ArchCUT3-D for micromorphological analysis. *Humanit. Soc. Sci. Commun.* 10 (1), 316. <https://doi.org/10.1057/s41599-023-01742-7>.
- Eymundsson, C., Fossum, G., Koxvold, L.U., Mansrud, A., Mjærum, A., 2018. Axes in transformation: a bifocal view of axe technology in the Oslo Fjord area, Norway, c. 9200–6000 cal BC. In: Glørstad, H., Knutsson, K., Knutsson, H., Apel, J. (Eds.), *The Technology of Early Settlement in Northern Europe. Transmission of Knowledge and Culture*, vol. 2. The Early Settlement of Northern Europe, Equinox, Sheffield, pp. 201–229.
- Galantucci, L.M., Grazia Guerra, M., Lavecchia, F., 2020. Photogrammetry applied to small and micro scale objects: a review. In: Ni, J., Majstorović, V.D., Djurdjanović, D. (Eds.), *Proceedings of 3rd International Conference on the Industry 4.0 Model for Advanced Manufacturing. Lecture Notes in Mechanical Engineering*. Springer International Publishing, pp. 57–77.
- Glørstad, H., 2002. Østnorske skafthullhakker fra mesolitikum. *Arkeologisk og forhistorisk betydning—illustrert med et eksempelstudium fra vestsiden av Oslofjorden*, vol. 65. Viking, pp. 7–48.
- Güth, A., 2012. Using 3D scanning in the investigation of Upper Palaeolithic engravings: first results of a pilot study. *J. Archaeol. Sci.* 39 (10), 3105–3114. <https://doi.org/10.1016/j.jas.2012.04.029>.
- Haaland, M.M., Strauss, A.M., Velliky, E.C., et al., 2021. Hidden in plain sight: a microanalytical study of a Middle Stone Age ochre piece trapped inside a micromorphological block sample. *Geoarchaeology* 36, 283–313. <https://doi.org/10.1002/gea.21830>.
- Hermon, S., Polig, M., Driessen, J., Jans, G., Bretschneider, J., 2018. An integrated 3D shape analysis and scientific visualization approach to the study of a Late Bronze Age unique stone object from Pyla-Kokkinokremos, Cyprus. *Digit. Appl. Archaeol. Cult. Herit.* <https://doi.org/10.1016/j.daach.2018.e00075>. S2212-0548(18)30003-1.

- Horn, C., Pitman, D., Potter, R., 2019. An evaluation of the visualization and interpretive potential of applying GIS data processing techniques to 3D rock art data. *J. Archaeol. Sci.: Reports* 27, e101971. <https://doi.org/10.1016/j.jasrep.2019.101971>.
- Horn, C., Ivarsson, O., Lindhé, C., et al., 2022. Artificial intelligence, 3D documentation, and rock art—Approaching and reflecting on the automation of identification and classification of rock art images. *J. Archaeol. Method Theor* 29, 188–213. <https://doi.org/10.1007/s10816-021-09518-6>.
- Lin, S.C., Rezek, Z., Dibble, H.L., 2018. Experimental design and experimental inference in stone artefact archaeology. *J. Archaeol. Method Theor* 25 (3), 663–688. <https://doi.org/10.1007/s10816-017-9351-1>.
- Marín-Buzón, C., Pérez-Romero, A., López-Castro, J.L., Ben Jerbania, I., Manzano-Agugliaro, F., 2021. Photogrammetry as a new scientific tool in archaeology: worldwide research trends. *Sustainability* 2021 (13), 5319. <https://doi.org/10.3390/su13095319>.
- Mélard, N., 2010. L'étude microtopographique et la visualisation 3D dans l'analyse de gravures préhistoriques — L'exemple des pierres gravées de La Marche. In *Situ*. <https://doi.org/10.4000/insitu.6837>.
- Mélard, N., Boust, C., Cogné, G., Maigret, A., 2016. Comparison of imaging techniques used in the microanalysis of Paleolithic mobiliary art. *J. Archaeol. Sci.: Reports* 10, 903–909. <https://doi.org/10.1016/j.jasrep.2016.05.038>.
- Meling, T., Fyllingen, H., Denham, S.D., 2020. Arkeologiske undersøkelser av bosetningsspor fra seinmesolitikum og tidligneoolitikum, samt aktivitetsspor fra bronsealder og førromersk jernalder (id 150773, id 150775, id 150776) på Sømme (Sømme III): Sømme gnr. 15, bnr. 161 m. fl. i Sola kommune, Rogaland fylke. Oppdragsrapport 2020/1. Universitetet i Stavanger Arkeologisk museum, Avdeling for fornminnevern.
- Milner, N., Bamforth, M., Beale, G., Carty, J., Chatzipanagis, K., Croft, S.C.K., Conneller, C., Elliot, B.J., Fitton, L.C., Knight, B., Kröger, R., Little, A.P., Needham, A., Robson, H.K., Rowley, C.C.A., Taylor, B., 2016. A unique engraved shale pendant from the site of Star Carr: the oldest Mesolithic art in Britain. *Internet Archaeol.* 40. <https://doi.org/10.11141/ia.40.8>.
- Molin, F., Gummesson, S., 2021. Dwellings and workspaces at Strandvägen, 5600–5000 cal. BC. *L'Anthropologie* 125 (4), 102926.
- Nami, H.G., 2010. Theoretical reflections on experimental archaeology and lithic technology. In: Nami, H.G. (Ed.), *Experiments and Interpretation of Traditional Technologies: Essays in Honor of Errett Callahan*. Ediciones de Arqueología Contemporánea, Buenos Aires, pp. 91–168.
- Nyland, A.J., 2016. *Humans in Motion and Places of Essence. Variations in Rock Procurement Practices in the Stone, Bronze and Early Iron Ages, in southern Norway*. Unpublished doctoral thesis. Department of Archaeology, Conservation and History, Faculty of Humanities, University of Oslo.
- Outram, A.K., 2008. Introduction to experimental archaeology. *World Archaeol.* 40 (1), 1–6. <https://doi.org/10.1080/00438240801889456>.
- Plonka, T., Diakowski, M., Krupa-Kurzynowska, J., Hoppe, V., Ziótkowski, G., 2023. Application of computed tomography to the study of Mesolithic portable art: results, interpretations and expectations—The case of an ornamented roe deer antler harpoon from Police, north-west Poland. *Archaeometry* 66 (1), 219–237. <https://doi.org/10.1111/arc.12904>.
- Radchenko, S., 2023. *Parietal and Portable Art of Kamyana Mohyla*. BAR Publishing, Ukraine. London.
- Radchenko, S., Kiosak, D., 2022. The Upper Paleolithic rock art of Ukraine between here and nowhere. *Quat. Int.* 640 (10), 44–60. <https://doi.org/10.1016/j.quaint.2022.09.008>.
- Radchenko, S., Nykonenko, D., 2019. Western edge of Steppe rock art. *Expression* 24, 49–62.
- Radchenko, S., Nykonenko, D., Kotova, N., Tuboltsev, O., Kiosak, D., Volkov, A., 2020. A complex rock art object in Ukrainian Steppe. *Rock Art Res.* 37 (2), 167–183.
- Rondini, P., 2018. Digital Rocks. An integrated approach to rock art recording: the case study of Ossimo-Pat (Valle Camonica), monolith 23. *Archeologia e Calcolatori* 29, 259–278. <https://doi.org/10.19282/ac.29.2018.21>.
- Skjelstad, G., 2003. *Regionalitet i vestnorsk mesolitikum. Råstoffbruk og sosiale grenser på Vestlandskysten i mellom- og senmesolitikum*. Upublisert hovedfagsoppgave i arkeologi. Universitetet i Bergen.
- Solheim, S., 2007. *Sørvest-Norge i tidligneoolitik tid: en analyse av etniske grenser*. MA-thesis in Archaeology. University of Bergen.
- van Gijn, A.L., 2010. *Flint in Focus: Lithic Biographies in the Neolithic and Bronze Age*. Sidestone Press, Leiden.